Bond hybridization and structural properties of clusters of group-IV elements

A. M. Mazzone
C.N.R., Istituto LAMEL, Via Gobetti 101, 40129 Bologna, Italy
(Received 1 October 1996; revised manuscript received 18 April 1997)

The aim of this study is twofold. Its central goal is to investigate the structural, energetic, and thermodynamic properties of homonuclear and heteronuclear clusters formed by elements with a different propensity towards s and sp bonds. The components of the homonuclear clusters are Al, Si, Ge, Sn, and Pb and heteronuclear clusters are Si and Ge clusters containing a fraction $\leqslant 0.5$ of one of the other elements. The cluster size is between 50 and 100. The second goal of our study is the comparison of well-established LCAO methods, of the *ab initio* and of the semiempirical type, in order to assess their limits in calculations of structures where size effects and heteronuclear bonding lead to hybridization of the electronic charge. The results indicate that, owing to the delocalized character of the p states and to the formation of complex $s\sigma$, $p\sigma$, and $p\pi$ bonds, the cluster structure is irregular. However, a general characterization as an aggregate of dimers is possible. The semiempirical methods are computationally much less demanding than the *ab initio* ones and the evaluation of quantities, such as the vibrational spectrum and the thermodynamic parameters, is possible even for medium to large size clusters. A major flaw of both the *ab initio* and the semiempirical methods is a remarkable dependence on the initial basis set. This, however, affects the quantities that depend on the details of the electronic charge. [S0163-1829(97)04347-6]

I. INTRODUCTION

In recent years, spurred by the need to identify unusual physical properties, there has been a massive effort towards the understanding of the properties of clusters. First-principles calculations have, to a large extent, focused on silicon, rare-gas, and alkali metals and, to a lesser extent, on noble-metal atoms. Many studies are also dedicated to van der Waals clusters whose stability arises from complex dissipative forces, such as H, He, and Hg clusters. The aspects of the cluster physics that have been generally addressed are (i) the ground-state geometry and its stability and (ii) the evolution of structural properties and of characteristic energies towards the bulk limit. Relatively little has been done to illustrate the property evolution with the atomic number and the same criticism applies to the thermodynamic properties and to the response to other energy inputs.

In spite of the very rich literature on Si clusters and on Si and Ge surfaces and interfaces, the elements of group IV still offer a challenge. For such elements, going down rowwise from Si, it is known that the sp^3 bond becomes an unfavored configuration and that the energies of the corelike d states represent a critical parameter in determining delicate structural energy differences.[1] Though these aspects have been examined in detail in solids and liquids, little progress has been made at the cluster level.

In addition to these speculative aspects, group-IV metallic elements (and specifically Sn) are being actively investigated for their application in sensor films, catalysis processes, and new cluster materials. For these applications generalizations of the cluster physics should be developed leading to a unifying view of the field.

However, the characterization of compound clusters is still in a very early phase and this, probably, reflects the absence of realistic potentials for many ordered and disordered alloys. The heterostructures more frequently investigated are bimetallic clusters where the alkali atom is the more abundant species. These applications are, however, sporadic and so are totally *ab initio* calculations. On the contrary, very detailed calculations have been developed in condensed phase chemistry for a variety of compound structures on the basis of the linear combination of atomic orbitals (LCAO) theory, so that the recourse to methods of this type is obligatory.

The purpose of this work is to analyze sp bonding more systematically than in Ref. 2. To represent electronic configurations with s, p, and d shells of increasing complexity the atoms forming the cluster are Al, Si, Ge, Sn, and Pb. The cluster structure is homonuclear, or heteronuclear of the type $Si_N A_x$, or $Ge_N A_x$, where A is Al, Sn, or Pb and x is a fraction $\leqslant 0.5$ of N. The properties that are addressed are the geometry, the characteristic energies, the vibrational spectrum, and the thermodynamic behavior. The study of the homonuclear clusters establishes the factors of charge hybridization arising from the atom type and from the cluster size and the heteronuclear clusters illustrate the effects due to the presence of heteroatoms. Furthermore, by their application to the characterization of the clusters, an attempt is made of a critical analysis of LCAO methods of different type.

The paper is organized as follows. In Sec. II the principles of some well-established LCAO methods of the *ab initio* and of the semiempirical type are briefly outlined. In Sec. III the properties of dimers and of clusters of size $N \leqslant 4$ are illustrated. The features of these small clusters serve as a guide to the characterization of the larger ones. In Sec. III a detailed comparison between numerical methods is also made. In fact the computer resources required for *ab initio* calculations of the heavier elements of group IV are substantial. This has limited the application of these methods to the clusters of the smaller size and all the results on the larger clusters have been obtained with a semiempirical method. In Sec. V the behavior of large (i.e., $N \sim 50,100$) homonuclear clusters is

analyzed with the attempt to tie their properties to the behavior of the smaller ones, the underlying physical assumption being that the large clusters are aggregate of dimers. In Sec. V a comparison is made between homonuclear and heteronuclear clusters. In this analysis we seek possible effects of segregation and/or the formation of stable endohedral locations. The main results are briefly summed and commented on in Sec. VI.

II. LCAO THEORIES: *AB INITIO* AND SEMIEMPIRICAL METHODS

Perhaps the most widely employed approximation for the calculations of molecular wave functions in quantum chemistry is that of the linear combination of atomic orbitals within the self-consistent field (SCF) framework.[3] An inherent difficulty of such calculations is that they require the calculation and subsequent manipulation of $\sim n^4$ two-electron integrals for a system containing n atomic orbitals. The n^4 catastrophe has prompted many researches to attempt to reduce the computer cost by using a clever mathematical expression or some form of neglect, or approximation, of the overlap integrals.

In the totally *ab initio* method of Dupuis and King[4] the program skips the computation of blocks of nonunique two-electron integrals thus forming a ''skeleton'' Fock matrix after which the true Fock matrix is generated by filling out the skeleton. In all the semiempirical calculations of the type modified neglect of the atomic orbital (MNDO) one- and two-center integrals of the Coulomb, hybrid, and exchange type are evaluated over orthogonalized atomic orbitals and are often approximated by a multicenter expansion. These integrals have an exponential form and contain some adjustable parameters. At the lowest level of refinement are the complete neglect of the differential orbitals (CNDO), the extended Debye-Hückel (EDH) being one of them. In EDH only the diagonal elements of the Fock matrix are calculated explicitly and the off-diagonal ones are obtained by the diagonal ones and by the experimental ionization potentials by using the Wolfsberg-Helmholtz or the Cusach's formula. Owing to this approximation, EDH is, by far, the most versatile and the fastest calculation. In the earliest days of the cluster chemistry EDH was widely used for the characterization of high-nuclearity clusters (references on these calculations can be found in the many studies of Mingos and his co-authors) and today is being used for exotic materials, such as molecular crystals of the BEDT-TTF type.

A wide body of studies, where the relative merits and failures of LCAO methods are analyzed, is available. For the purpose of this study it is recalled that a problematic aspect is their dependence on the initial basis set so that relative results are often of more significance than absolute results. This problem is, however, shared by refined quantum mechanical methods, such as the ones of the Monte Carlo type, and by the local density approximation (LDA).

The packages HONDO,[5] MOPAC,[6,7] and EHA (Refs. 8 and 9) have been used for Dupuis, MNDO, and EHD calculations, respectively. The basis functions available in HONDO are of Slater type (STO), Gaussians (6-21G,6-31G), Dunning's $(9s,5p)$ (DZ), and effective core potential (ECP). Both DZ and ECP functions may have double or triple ζ quality (indicated as ECDP).

While in HONDO each electron shell, including the inner ones, is resolved into its atomiclike components; in MOPAC only valence electrons are treated explicitly by using s- and p-type orbitals. This does not allow a clear identification of the d-shell contributions. In EHA a STO basis is used and the parameters of these functions represent s, p, d, and f atomic shells. In HONDO and MOPAC SCF calculations are coupled with geometry optimization. EHA does not offer this possibility. Consequently in our study EHA has been applied to the optimum geometry calculated by MOPAC or HONDO.

In HONDO and MOPAC either unrestricted, multiconfigurational, or aufbau SCF calculations can be performed. The calculations for clusters of size $N \leqslant 4$ are of the former type whereas for the larger clusters only aufbau calculations were practically feasible. Furthermore MOPAC contains three different semiempirical Hamiltonians (MNDO, AM1, and PM3), which differ for the parametrization of the core integrals. A detailed comparison of these Hamiltonians has been presented in Ref. 2. MNDO has been parametrized for all the atomic species used in this study and for this reason has been adopted here. The results reported in paragraphs 5 and 6, unless otherwise specified, are MNDO calculations.

An important feature of LCAO methods is that they allow the straightforward evaluation of the vibrational spectrum and of the related thermodynamic properties, as these quantities can be obtained from the eigenvalues of the Hessian matrix for the most stable configuration. However, the extrapolation of these results to the configurational space near a phase change is doubtful and in the calculations presented in the following paragraphs the changes of entropy are used to signal, only in qualitative terms, a change of the melting behavior.

It is known that the potential energy surface of a cluster has an extremely large number of local minima. For Lennard-Jones clusters, for instance, it has been evaluated that such minima are 147 for the size $N=32$ and their number increases to 10^7 for $N=100$. Under such conditions the search for a minimum is obviously biased by the type of structure that one wishes to investigate. Similarly to the criteria used in Ref. 2, in this series of calculations the minimization was started with a distorted fullerene cage.

Where possible, the results have been compared with other theories and with experiments. However, this comparison is in practice limited to Si and Al as very few other sources of comparison seem to be available.

III. TRENDS IN BONDING: DIMERS AND SMALL CLUSTERS

The homonuclear clusters to be examined in this sections and in the following ones are formed by Al, Si, Ge, Sn, and Pb (this order, which follows the increase of the atomic number, will be generally maintained in the presentation of the data). Heteronuclear clusters are Si and Ge clusters with substitutional Al, Ge, Sn, and Pb. In the following, Si and Ge are indicated as the semiconductor element and Al, Sn, and Pb, rather loosely, as the metallic element. In structures of the type Si-Ge the S and M elements are Si and Ge, respectively. The cluster structure obtained from the static energy minimization is hereinafter defined, according to the literature on metallic clusters, as the best single cluster (BSC). The bind-

ing energies, the highest occupied molecular orbital–lowest unoccupied molecular orbital (HOMO-LUMO) gap, and the eigenenergies of the BSC configuration, reported in the following figures and tables, indicate the absolute value of these quantities.

The configuration of the valence electrons and of the nearest inner subshells of the atoms forming the clusters is $3s(2)3p(1)$ for Al, $3s(2)3p(2)$ for Si, $3d(10)4s(2)4p(2)$ for Ge, $4d(10)5s(2)5p(2)$ for Sn, and $5d(10)6s(2)6p(2)$ for Pb. In group IV the bond order coefficient for a sp^3 bond decreases from about 14 to 6 in passing from Si to Pb (Ref. 1) and in the corresponding set of solids at room temperature

TABLE I. The data illustrate the bonding in dimers. R_b and E_b indicate the average bond length and the binding energy per atom, respectively. HL is the width of the HOMO-LUMO gap, and $f_{\max}$ is the frequency of the dimer vibration. $R_{\rm nn}$ and $E_{\rm coh}$ are the nearest-neighbor distance and the cohesive energy, respectively, in the solids. In (b) the S and M charges represent the change of the electronic charge on atom and are evaluated from the Mulliken population analysis. An omitted column indicates that the quantity is not available by using the given method.

(a) Homonuclear dimers

Hamiltonian	Basis	Dimer	R_b (Å)	E_b (eV)	HL (eV)	$f_{\max}$ ($\rm cm^{-1}$)	$R_{\rm nn}$ (Å)	$E_{\rm coh}$ (eV)
HONDO	STO	Al2	2.81	0.45			2.35	3.34
		Si2	2.25	2.15			2.32	4.83
		Ge2	1.84	3.14			2.44	3.85
		Sn2	2.23	2.39			2.80	3.14
	6-31G, ECDZ	Si2	2.34	1.49				
	ECDP ECDZ	Ge2	2.21	1.04				
		Sn2	2.79	1.47				
		Pb2	2.88	1.23			2.80	2.06
MNDO	s,p	Al2	2.40	0.80	3.13	356.0		
		Si2	1.98	1.19	5.33	539.0		
		Ge2	2.03	0.99	6.07	281.0		
		Sn2	2.40	2.34	4.92	257.0		
		Pb2	2.54	1.65	4.81	171.0		
EHA	STO	Al2	2.40	1.70				
		Si2	1.98	4.19	1.94			
		Ge2	2.03	3.95	1.40			
		Pb2	2.54	3.66	1.19			

(b) Heteronuclear dimers

Hamiltonian	Basis	Dimer	R_b (Å)	E_b (eV)	HL (eV)	$f_{\max}$ ($\rm cm^{-1}$)	S charge	M charge
HONDO	STO	SiAl	2.32	1.35			−0.02	0.02
		SiGe	2.23	2.69			−0.32	0.40
		SiSn	2.42	2.54			−0.37	0.37
		GeSn	2.38	2.71			−0.10	0.10
	ECDP	SiAl	2.65	1.12				
		SiSn	2.52	1.63			0.05	−0.05
		SiPb	2.52	0.30			0.05	−0.05
		GeAl	2.72	1.07			−0.01	0.01
		GePb	2.64	1.49			−0.01	0.01
MNDO	s,p	SiAl	2.18	1.04	2.98	435	−0.05	0.05
		SiGe	1.91	0.97	5.23	393	−0.40	0.40
		SiSn	2.22	1.61	5.10	408	0.19	−0.19
		SiPb	2.32	1.61	5.05	360	0.29	−0.29
		GeAl	2.37	0.92	3.05	319	0.17	−0.17
		GeSn	2.17	1.57	5.01	272	0.37	−0.37
		GePb	2.44	2.43	4.95	232	0.47	−0.47
EHA	STO	SiAl	2.18	4.65	1.91		−0.92	0.92
		SiGe	1.91	4.50	2.07		−0.20	0.20
		SiPb	2.23	3.86	1.54		−0.75	0.75

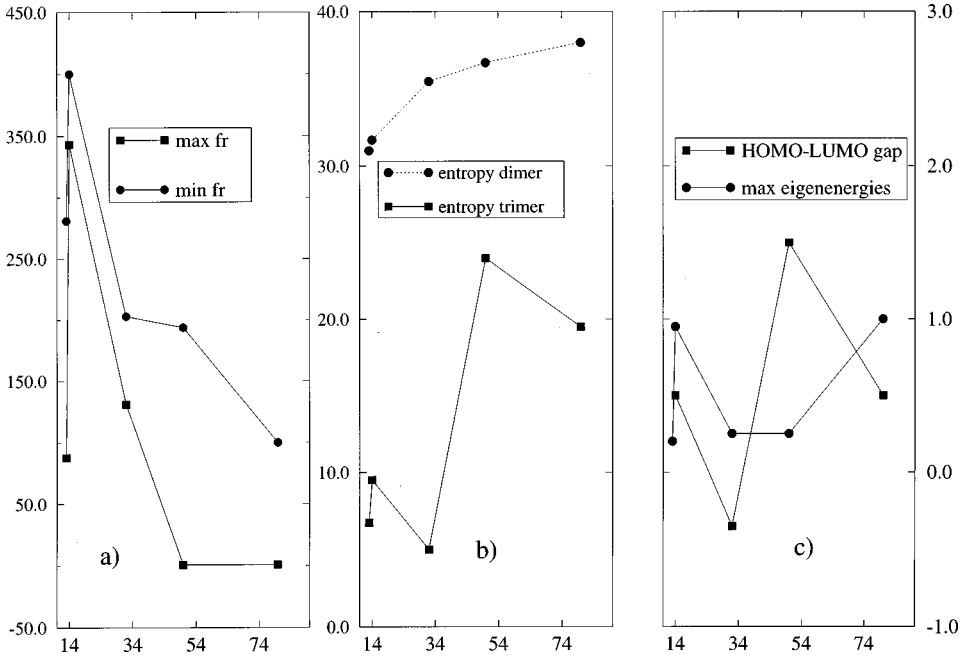

FIG. 1. Properties of trimers as a function of the atomic number. The panel (a) shows the maximum and the minimum value of the spectrum of the vibrational frequencies. The frequencies are measured with respect to the dimer frequency $f_{\max}$ reported in Table I(a). The unit of measure of the frequencies is cm^{-1}. The panel (b) shows the entropy of dimers and trimers. The entropy of trimers is measured with respect to that of dimers. The unit of measure of the entropy is cal/K. The panel (c) reports the HOMO-LUMO gap and the maximum values of the eigenenergies measured from the dimer values. For both graphs the unit of measure is eV.

the structure changes from a tetrahedral coordination with a bond length around 2.3 Å and a bond angle around $\sim 103°$ to a fcc structure with a longer bond distance ~ 3.0 Å and a smaller bond angle of value $\sim 60°$. Furthermore the property of silicon to form distorted bonds and polymorphic structures with a minimum promotion energy is one of the more frequently investigated effects of solid state physics. Most of the features reported below reflect some of these properties of the atoms and of the solids.

Table I(a) and (b) illustrates the main properties of homonuclear and heteronuclear dimers. From Table I(a) it is seen that the bond length R_b and the binding energy E_b of homonuclear dimers (fourth and fifth columns) are shorter and smaller, respectively, than the nearest-neighbor distance R_{nn} and the cohesive energy E_{coh} in the solids [last two columns in Table I(a)]. Furthermore the analysis of the electronic shell structure (not reported in the table) indicates that the charge distribution becomes more spherical and its orientation along the dimer axis (labeled x) disappears as the atomic number of the element increases.

For dimers of all types the prevailing components of bonding are $p\sigma$ and $p\pi$. Consequently the covalent charge is distributed in orbitals that point along the bond and also in orbitals in planes perpendicular to the bond. The dipole moment of homonuclear dimers is inappreciable and their vibrational spectrum has only one radial σ_g mode. In the crystals the frequency of the TO mode has values of 517, 278, and 186 cm^{-1} for Si, Ge, and Sn, respectively.[10] As shown in Table I(a), the MNDO dimer frequency, with the exception of Sn, is very close to these values.

The calculations indicate that the shape of BSC of homonuclear trimers and tetramers has a remarkable dependence on the Hamiltonian. Generally, however, the trimers of Al, Si, and Ge have a symmetric linear arrangement along x and this structure arises from the preferential orientation of the electronic charge along x. In Sn and Pb the weakness of the p_x bond and its spread into p_y and p_z components lead to a triangular shape. The triangle is irregular and the two bond lengths may be remarkably different. For Al, Si, and Ge this growth pattern, in which the number of the nearest-neighbor distance is maximum, clearly appears only at the size $N=4$. For these elements the tetramer structure is a distorted pyramid while either a plane rhombus or a pyramid has been found for Sn and Pb.

The bond length distribution within trimers and tetramers leads to the formation of a richer spectrum, with respect to the dimer case, of either the vibrational frequency or of the eigenenergies. It has been experimentally shown, in fact, that the low frequency side of the spectrum of large clusters arises from undercoordinated atoms and, generally, from the formation of a bond length distribution.[11] These effects are illustrated in Fig. 1. The graphs in the figure plot (i) the maximum and the minimum frequency of the vibrational spectrum, (ii) the entropy, (iii) the maximum value of the electronic energy in the molecular orbitals, and (iv) the width of the HOMO-LUMO gap.

These parameters are not physically homogeneous. In fact, while (i), (iii), and (iv) depend on the distribution of ''soft'' and ''strong'' bonds in the cluster, the entropy depends on the nearly isomeric structures available in the vicinity of BSC and reflects the propensity to fill the phase space under the effect of a temperature increase. All the parameters, unless otherwise specified, refer to the size $N=3$ and are measured with respect to $N=2$ so that they are illustrative of the changes due to the addition of one atom to the dimer. The figure shows the dependence of this increase on

the atomic number Z. This Z dependence is, however, peculiar to small structures as it has been observed also in passing from N to $N+1$, or to $N+2$, with $N=2,3$.

The notable feature of these calculations is the homogeneous behavior of Ge, Sn, and Pb while Si appears anomalous with respect to its cogener elements and its behavior has some more affinity with Al. For Ge, Sn, and Pb it is seen that the frequency spectrum has a smaller change, with respect to the dimer frequency, than Al and Si. Furthermore their entropy and their eigenenergies have a similar monotonous increase with Z. The similarity between the Z dependence of the entropy and of the HOMO-LUMO gap is underlined. A simple understanding of this result comes from the similarity of the spectra of vibrations and of eigenenergies. This aspect, however, has not been fully analyzed.

The heteronuclear configuration [Table I(b)] shows significant changes of the dimer structure and its characteristic energies. The electron-rich bond due to the presence of the M atom leads to an increase of binding, even if the diffuse orbitals on the M side lead to the increase of the bond length. Such hybridization has a modest effect on the width of the HOMO-LUMO gap as the two energies across the gap are a complex combination of bonding and antibonding states and effects of charge redistribution nearly cancel. Owing to the charge exchange between the S and M atoms, the bonding in SM dimers acquires a partially ionic character. In SiM the maximum frequency is noticeably reduced with respect to Si2. In GeM this reduction takes place only if M is Sn or Pb. This dependence on Z is similar to that of homonuclear dimers and characterizes the vibrations of the dimers as the ones of a classic, harmonic oscillator. The increase of E_b, which is signaled by almost all methods, shows the formation of ''ligand effects'' in SM with respect to SS or MM. In chemistry such ''ligand'' effects are amply made use of. In such cases, however, it is generally a CO, or CH, complex that acts as a ligand in a cluster of metallic atoms. Some reversal of this role is observed in SM dimers.

HONDO, MNDO, and EHA lead to a consistent picture of the qualitative features, summarized above. However, as shown by the data, the quantitative discrepancies are not secondary and indicate well-defined propensities of the calculations. The fluctuations of R_b due to the use of HONDO or MNDO are in the range 20%. Differences of the same amount have been also found for the clusters of size $N \leqslant 5$ of all five elements and for larger clusters ($N \sim 10$) of Al. These results suggest that the cluster geometry is consistently evaluated by the two methods and the fluctuations of the geometrical parameters are in the range 10%.

The evaluation of the binding energy and of the electronic charge shows a critical dependence on the initial basis set. The use of the simple STO basis set, either in HONDO or EHA, appears to underestimate the internuclear repulsion and the electron-nuclear attraction. Consequently the binding energies are large and in some cases (for instance, EHA Pb2) a dubious growth of E_b above $E_{\rm coh}$ is observed. Conversely, the S and M charges of heteronuclear dimers [last two columns in Table I(b)], evaluated with STO, have the reverse sign than in the other calculations.

In HONDO calculations with the ECP basis, the inner-shell electrons are treated within the effective-core approximation. This is conceptually similar to MNDO, as in MNDO only valence electrons are treated explicitly, and this accounts for the similarity between the two sets of data. However, the ratio Q_{sp} between the s and p charges of homonuclear dimers in MNDO is 0.81 for Si2 increasing to 1.114 for Pb2, this increase being due to the decrease of the p charge. In HONDO with ECP basis the electronic charge has a stronger localization in the p shells. Consequently, Q_{sp} is more homogeneous and its values oscillate only between 0.97 and 0.95. This charge distribution accounts for the lower charge exchange found in heteronuclear dimers when using HONDO ECP.

However, the problematic aspects of carving the Mulliken charge, or the similar, from the electron density distribution are known and may occur also using the LDA formulation.[12] In our case the charge exchange between heteroatoms is small and depends on the details of the electron wave functions at the extremity of the bond. This enhances the critical character of its evaluation.

To compare the results of this paragraph with similar ones reported through the literature, we recall that the E_b values of Si and Al dimers obtained from LDA and *ab initio* calculations are in the range 1.56–1.8 eV and 0.26–1.4 eV, respectively. The corresponding R_b values are 2.23 and 2.15–2.98 Å (see Refs. 2 and 13). For the Ge dimer the value of R_b and of $f_{\rm max}$ is 2.45 Å and 240.0 $\rm cm^{-1}$, respectively, in Ref. 14. These data, globally considered, suggest that the quantitative differences between these theories and MNDO should fall in the range $\sim 20-30\%$.

On a more qualitative ground, in agreement with the calculations in Ref. 15, which indicate that the two atoms are compatible from both points of view of the size and of the electronic configuration, the properties of SiAl are, in our calculations, the closer ones to Si2. Furthermore there is consistency between the MNDO thermodynamic data and the data on melting available in the literature. In fact, the values of the entropy per atom of homonuclear dimers [reported in panel (b) in Fig. 1] are two orders of magnitude smaller than the ones calculated for Ar3 in Ref. 16 using methods based on classical molecular dynamics and Liapunov exponents. This difference is consistent with the difference of the melting temperatures of the corresponding solids.

IV. HOMONUCLEAR CLUSTERS

The analysis of the size dependence of the binding energy of homonuclear clusters showed a sharp increase of this parameter over the dimer value for the size $N \geqslant 10$ followed by a saturating behavior for N in the range 40. This paragraph sums up the properties of this group of large and stable clusters. These clusters do not possess the symmetry properties that are peculiar, for instance, of carbon, or of some transition-metal atom clusters. Consequently they cannot be characterized on the basis of spatial and vibrational symmetry groups but with reference to their simpler constituents, i.e., clusters of a smaller size.

A. The geometry: The binding energy

It is known that the stability of large clusters arises from the formation of manyfold coordinated atoms (a detailed bibliography on Si clusters has been presented in Ref. 2). Con-

TABLE II. The quantities reported in the table are the binding energy per atom (E_b), the maximum and minimum cluster size (R_{max} and R_{min}, respectively), the average bond length (R_b), the average bond angle (Θ), and the coordination (Coor). R_b and Θ refer to the central atom in the cluster. Coor represents the number of atoms within a sphere of radius R_{cut}. R_{cut} is 3.0, 2.4, 2.4, 2.8, and 3.0 Å for Al, Si, Ge, Sn, and Pb.

Homonuclear clusters						
Cluster	E_b (eV)	R_{max} (Å)	R_{min} (Å)	R_b (Å)	Θ	Coor
			Elongated			
Al40	1.89	16.10	9.01	2.80	101.0	4.60
Si89	4.28	21.96	9.42	2.27	106.0	2.84
Ge89	2.80	23.36	10.04	2.75	96.30	2.18
Sn40	4.40	13.84	8.50	2.64	109.0	3.75
Pb48	3.30	19.20	7.73	2.89	103.0	3.71
			Spherical			
Al72	2.01	15.21	12.74	3.31	91.50	4.00
Si72	4.90	11.75	10.59	2.44	101.0	3.22
Ge72	3.17	13.32	12.62	2.62	99.00	2.14
Sn72	4.85	13.03	11.72	2.86	93.50	6.20
Pb50	3.52	11.50	9.51	3.03	102.0	4.32

versely, the similarity of the σ and π bond components with the ones in the dimer configuration becomes progressively blurred as the overlapping of the charges of neighboring atoms increases with the increase of their coordination. In dimers the largest diagonal term of the bond-order matrix is of the $p\pi$ type and its value is equal to 1.0 in Si, Ge, Sr, and Pb. The next largest one is $p\sigma$ and its value is 0.947, 0.71, 0.79, 0.97, and 0.97 in Al, Si, Ge, Sn, and Pb, respectively. At variance with these data, in the large clusters the $p\pi$ and $p\sigma$ components may fluctuate between 0.5 and 2.5 and also a $s\sigma$ component as large as 0.9 has been observed in Si. Consequently structured shapes, with a wide distribution of bond angles and lengths, are expected to be peculiar of these clusters.

The main parameters of the cluster geometry and their binding energy are shown in Table II. In Ref. 2 it has been shown that large clusters of Si, Ge, and Pb may have either a spherical or an elongated structure and that Si and Ge clusters contain manyfold coordinated atoms in rings of an approximate wurtzite type. The cluster dimensions R_{max} and R_{min}, reported in Table II, indicate that the spherical and the elongated structure (indicated in the following as SP and E, respectively) are also possible for Al and Sn. Furthermore R_{max}, R_{min}, and the eccentricity ratio R_{max}/R_{min} are similar for the five elements though some fluctuations in the E group and more homogeneity in the SP one are observed.

The systematic analysis of the M elements of group IV indicated that the diffuse character of their p charge leads to the disappearance of the rings observed in Si and Ge. However, as shown by the values of the average coordination in Table II, also the metallic clusters achieve a high compactness and the geometrical factor leading to this behavior is the sharing of triangular or pyramidal elements. Fused pyramidal or triangular elements are reminiscent of a ring of atoms, the main difference being that in the ring the capping atoms are missed. This feature accounts for the similarity of the structure and of the dimensions of Sn and Pb, on one side, and Al, Si, and Ge, on the other side. For Al the absence of an icosahedral pattern is consistent with the size being removed from the magic numbers for icosahedral growth and is also in agreement with more recent results on amorphous Al and Au clusters.[17]

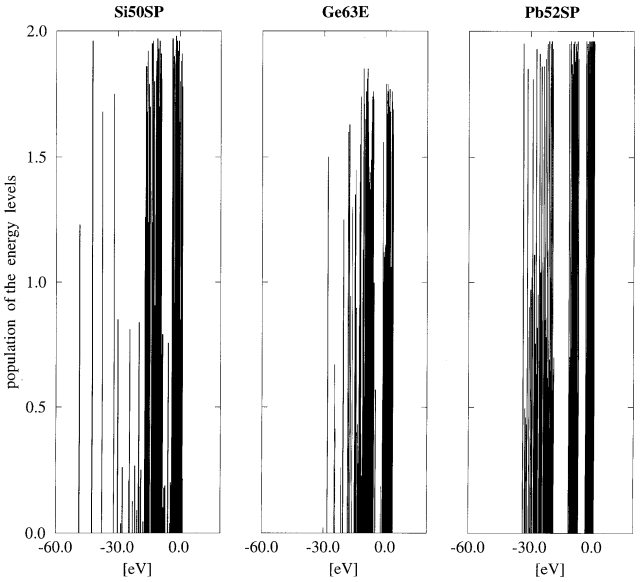

FIG. 2. The electronic configuration of homonuclear clusters. The figure shows the eigenenergies and the population of the energy levels for Si50SP, Ge63E, and Pb52SP.

The charge overlapping mentioned at the beginning of the paragraph leads to a remarkable increase of bond angles and lengths over the dimer values. In the elongated clusters R_b increases above the dimer value of $\sim$20% and the increase may be as large as 40% in the spherical ones. Furthermore, almost in all cases, the average bond angle Θ changes from the small value, typical of the equilateral triangle, to the value required by tetrahedral coordination.

The E_b values of Al, Si, and Ge closely follow the trend of the bulk cohesive energy (reported above in Table I) while E_b of Sn and Pb appear to be overestimated with respect to E_{coh}. As discussed in Ref. 2, this effect is attributable to the parametrization of the Hamiltonian. However MNDO geometries appear to be consistent with LDA calculations of Si and Al. In fact, the eccentricity ratio and the average bond length for Si70 in Ref. 18 are 1.3 and $\sim$2.44 Å, respectively, and the corresponding MNDO values are 1.01 and 2.44 Å. In Ref. 20 the values of E_b and R_b for Al13 are 2.29 eV and 2.57 Å. The corresponding HONDO and MNDO values are 2.38 eV, 2.30 Å and 1.89 eV and 2.54 Å, respectively. This comparison leads to an acceptable agreement between MNDO and other results. However, in Ref. 19, on the basis of an EAM potential, a value equal to 2.84 eV has been obtained for E_b of Al55. This value is remarkably larger than our evaluation of binding in Al.

B. The spectra of the electronic energies and of the vibrational modes: The thermodynamic properties

As for dimers, we characterize the bond-length distribution within the clusters through its effects on the electronic energy spectrum and on the distribution of the vibrational modes.

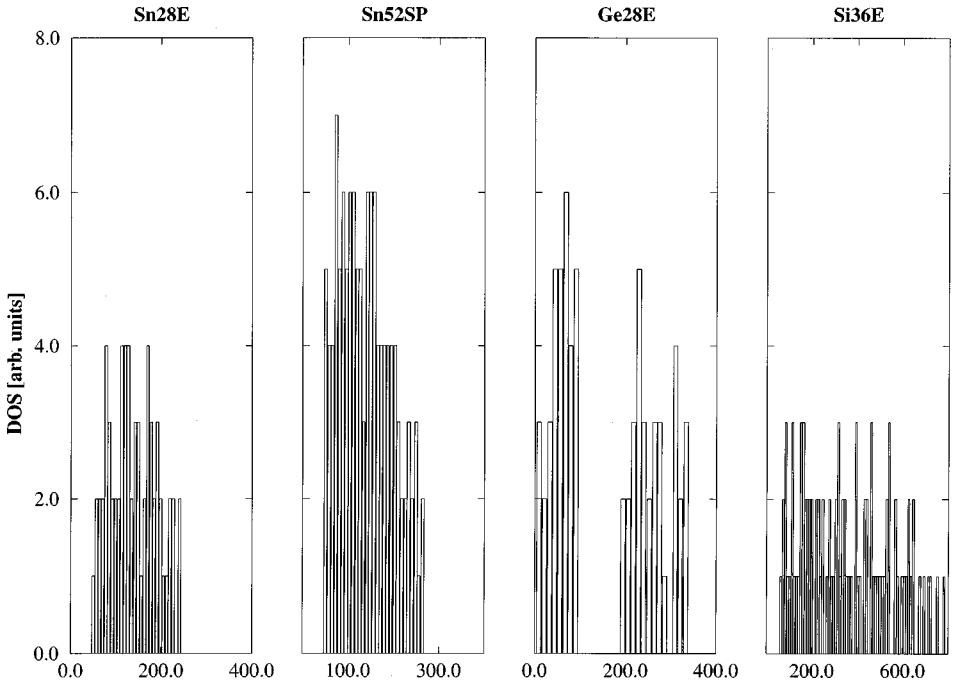

FIG. 3. The vibrational spectrum of homonuclear clusters. The figure shows the distribution of eigenmodes of Sn28E, Sn52SP, Ge28E and Si36E. The unit of measure of the frequencies is cm^{-1}.

Representative plots of these two quantities, for different cluster geometry and atom type, are reported in Figs. 2 and 3 and they both indicate a variety of bonding configurations within the cluster. The graph of the electronic energies of the molecular orbitals (Fig. 2) shows mixed features containing isolated levels and bandlike structures and the complexity of the spectrum appears to increase in the reverse order of the atomic number.

The typical vibrational spectrum of an amorphous material consists of two main broadbands centered around the TA and TO frequencies and in a crystal several satellite peaks are distributed between these two peaks. Evidently neither of these models is fitting with the cluster behavior (Fig. 3), which consists of many, nearly equispaced, normal modes and single breathing modes. As shown by the comparison of Sn28E and Sn52SP, the number of normal and single modes and their maximum degeneracy increases with the cluster size. Though the mode distribution has a significant dependence on the cluster size, the increase of the bandwidth is marginal and the calculations indicated that the bandwidth of

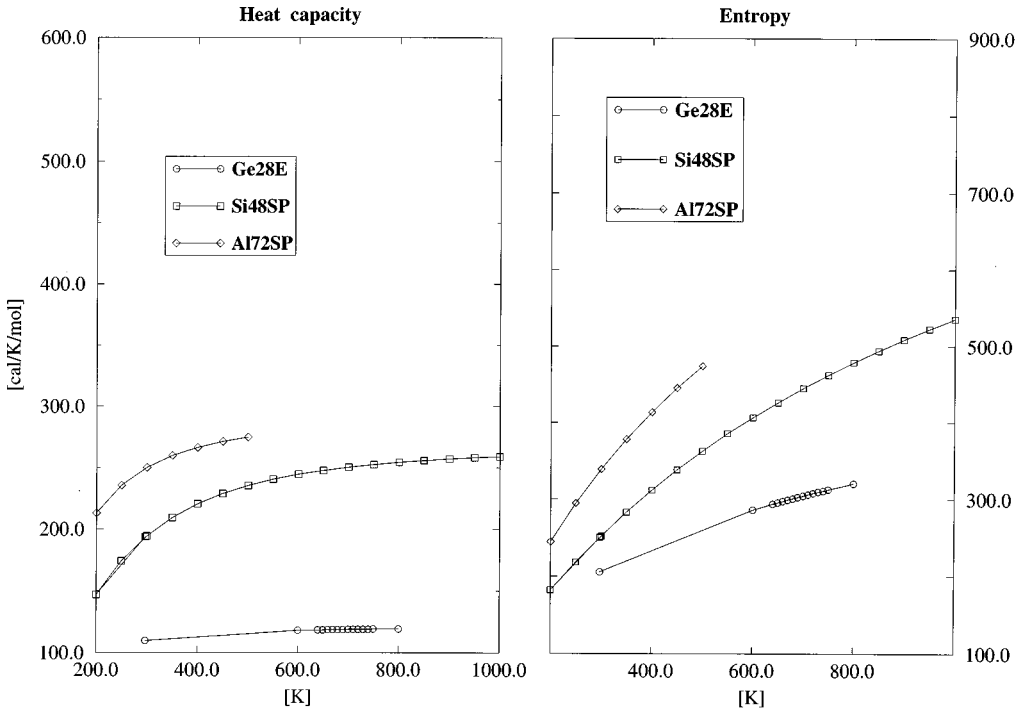

FIG. 4. The temperature dependence of the heat capacity and of the entropy per atom.

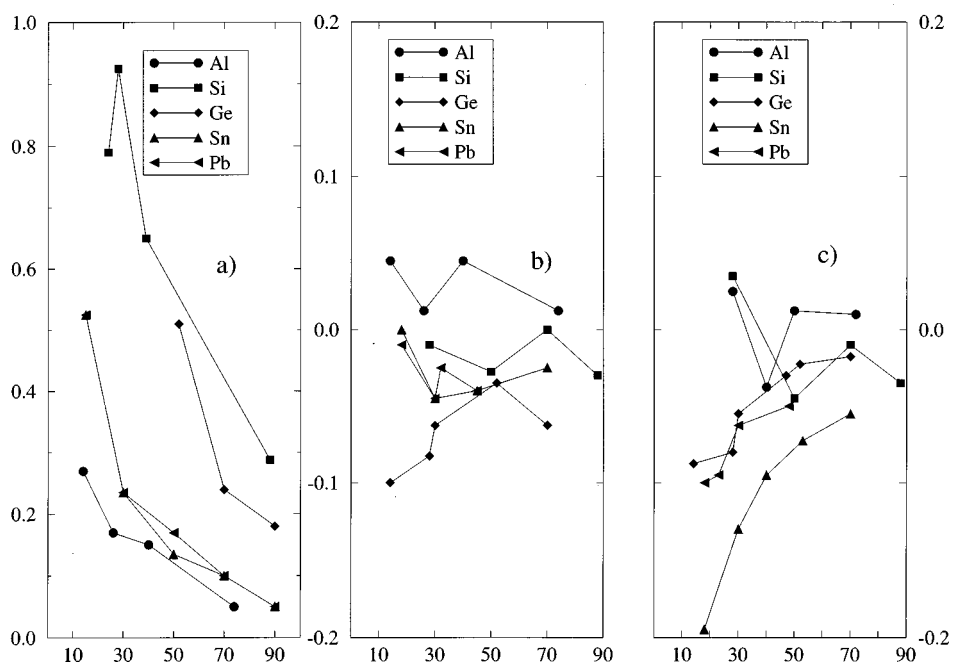

FIG. 5. Properties of clusters as a function of the cluster size. The panel (a) shows the maximum values of the eigenenergies measured from the dimer values. The panel (b) shows the HOMO-LUMO gap measured from the dimer values. The panel (c) shows the HOMO-LUMO gap measured from the trimer values. In (a), (b), and (c) the unit is eV.

trimers represents an acceptable approximation for clusters of all sizes. In agreement with this conclusion, it has been shown in Ref. 21 for Ni clusters of size $N \leqslant 55$ that the width of the modes distribution and their maximum frequency is independent on N.

In Fig. 4 the temperature dependence of the heat capacitance and the entropy is reported for different atom types and cluster sizes. Somewhat in conflict with the irregular structure of the energy and of the vibrational spectrum, the entropy appears to be governed by a regular assembly of harmonic oscillators and its behavior is of the Einstein-Debye type, with a nonzero value at room temperature. This indicates that only some ''effective'' modes control the thermodynamic behavior. Furthermore the comparison of smaller and larger clusters indicates a nearly linear decrease of the entropy with N. This is in agreement with the increase of the melting temperature with N, a behavior known since early studies on clusters.[22]

Owing to the absence of clear structural effects on the vibrational spectrum and on the characteristic energies, an attempt has been made to tie these properties to the ones of dimers. Representative calculations are reported in Fig. 5. These calculations refer to two parameters of the energy spectrum, i.e., (i) the maximum value of the spectrum of the electronic energies and (ii) the width of the HOMO-LUMO gap. The graphs in Fig. 5 report the increase per atom of (i) and (ii) above the dimer value. For (i) [Fig. 5(a)] it is seen that the difference with respect to the dimer is small and tends to decrease with the increase of the size N. Evidently, the charge in these deeply bonded states retains the s quality of dimers and the cluster can be characterized as an aggregate of dimers. On the contrary, the width of the HOMO-LUMO gap [Fig. 5(b)] does not offer such a simple interpretation as the difference with respect to dimer fluctuates irregularly with the size. However, if the HOMO-LUMO gap of the tetramers is taken as a reference [Fig. 5(c)] the behavior becomes even more irregular and the dimer seems to offer a more valid approximation.

From the comparison of these results with the ones reported in the literature discrepancies and similarities have emerged. In fact the LDA evaluation of the HOMO-LUMO gap for Si70 in Ref. 18 is around 0.9 eV, which is considerably lower than MNDO results but is quite close to the EHA values of Table I. In MNDO calculations Ge28E has two well resolved peaks at $\sim 80\ \mathrm{cm}^{-1}$ and $\sim 269\ \mathrm{cm}^{-1}$, respectively, and this is in good agreement with the Raman spectrum of amorphous clusters reported in Ref. 11. Furthermore the spectrum of vibrational frequencies of Si36SP, obtained from MNDO, has a near uniform distribution of peaks. A similar spectrum has been evaluated in Ref. 23 for two clusters of similar size, i.e., Si20 and Si21. The maximum frequencies of these clusters are, however, noticeably lower than ours (i.e., $\sim 450\ \mathrm{cm}^{-1}$ in Ref. 23 and $\sim 600\ \mathrm{cm}^{-1}$ in MNDO calculations).

V. HETERONUCLEAR BONDING: HETERONUCLEAR CLUSTERS

A subtle point in cluster studies is that the similarity with the atomic orbitals is lost and consequently properties such as covalency, ionicity, and bond hybridization are not simply defined and even less quantified. For this reason the characterization of heteronuclear clusters is by necessity simple and we analyze only the effects due to the different electronic structures of the S and M element and the ones due to the the cluster size. Even with this reduced emphasis the two aspects are not easily disentangled. However, in this paragraph an attempt is made to sever their role.

TABLE III. In the table the *S* and *M* charge represent the average change of the electronic charge on atom and are evaluated from the Mulliken population analysis. *SM*, *SS*, and *MM* bonds are the number of atoms (fraction of the total) of the *S* and *M* type that have a nearest neighbor of the *M* and *S* type within a sphere of radius 2.4 Å. Atoms having either an *S* or an *M* neighbor are double counted.

			Heteronuclear bonding			
Cluster	*M* atom fraction	*S* charge	*M* charge	*SM* bond	*SS* bond	*MM* bond
			Silicon			
48*E*	0.38 Al	0.64	−1.08	0.92	0.73	0.12
48*E*	0.54 Pb	0.12	−0.104	0.92	0.35	0.31
48*E*	0.41 Ge	−0.55	0.77	0.75	0.58	0.17
89*E*	0.41 Sn	0.33	−0.46	0.87	0.27	0.01
89*E*	0.41 Al	1.14	−1.61	0.84	0.25	0.10
50*SP*	0.28 Al	0.59	−1.52	0.60	0.88	0.07
			Germanium			
28*E*	0.39 Al	1.19	−1.84	0.29	0.68	0.14
89*E*	0.25 Pb	0.28	−0.88	0.14	0.48	0.04
49*SP*	0.41 Al	1.35	−1.96	0.73	0.28	0.14

A. Heteronuclear bonding

In recent years some contradictory indications on clustering of heterogeneous atoms have emerged. Studies of fullerene cages have, in fact, shown that endohedral locations are stable also for a high degree of vibrational excitation of the atoms of the cage. In a very detailed study of alkali-lead compounds[24] it has been shown that in a network of Pb4 tetrahedra K atoms are located in the large holes of this network. The reversal of the cluster composition leads to similar results. In fact, peculiar endohedral locations of Pb in Na clusters have been shown to exist experimentally and theoretically.[25] On the contrary, in Ni clusters Al heteroatoms may segregate at the surface or be located in the central site of the cluster,[19] depending on the cluster size. Furthermore studies of metal/silica nanostructures have shown that domains are formed that are enriched with one or the other of the two components and are separated by a sharp interface.[26]

This state of the art indicates that either the formation of stable endohedral locations or segregation is possible and these effects have a subtle dependence on the chemistry of the system concerned. To investigate the propensity for one or the other possibility we sought the most stable position of an *M* monomer, or dimer, within a small cage of the *S* element (Si13 and Ge13). The results indicated that the stable location of the isolated atom is displaced from the baricenter of the cluster and, generally, corresponds to the heteroatom being maximally coordinated. In small clusters, with a large fraction of surface atoms, this may lead the heteroatom to segregate at the surface. Furthermore, for an *M* dimer, there is no tendency of the two *M* atoms to stick together. On the contrary, each of them separately replicates the behavior of the isolated atom and attempts a maximum coordination with the *S* cage.

These trends are obviously more complicated in large clusters containing a sizable fraction of the *M* element; in such cases a network of *M* atoms can be formed by proximity effects. However, even in those cases the analysis of the coordination clearly showed a tendency towards maximum coordination through heterobonding. These data are reported in Table III. For a stoichiometry ratio $M/S \leqslant 0.5$ the large fraction of *SM* bonds indicates that there is no tendency towards the segregation of the element *S* from *M*. A further important result is that the charge retains the main character of the *SM* dimer. In fact the charge transfer takes place

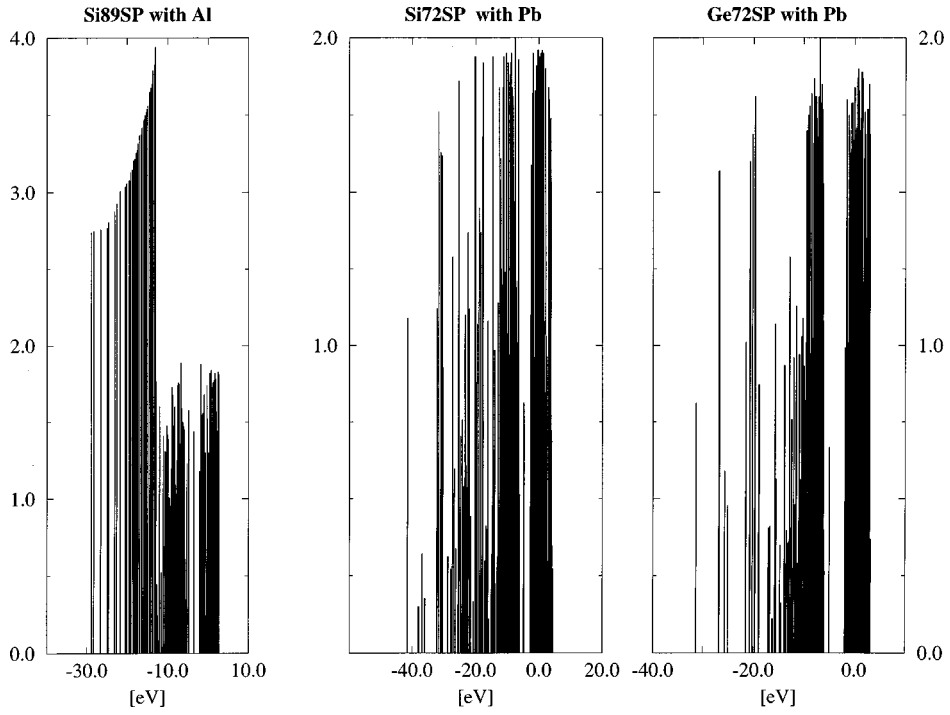

FIG. 6. The electronic configuration of heteroclusters. The figure shows the eigenenergies of the molecular orbitals. Si89*S* with 37 Al atoms, Si72*S* and Ge72*S* with 31 Pb atoms.

TABLE IV. Heteronuclear *SM* clusters. Properties of the *S* and *M* component. The parameters reported in the table are the binding energy E_b per atom measured with respect to one semiconductor plus a metallic atom, R_b and Θ are the average bond length and angle for the two components of the cluster. The ''covalent,'' ''metallic,'' and mixed type of bonding are indicated. The values of R_b and Θ where a more remarkable change with respect to the homonuclear case has been observed are marked in bold.

			S element		*M* element	
Cluster	Metal fraction	E_b (eV)	R_b (Å)	Θ	R_b (Å)	Θ
			Silicon			
			Covalent bonding			
			Al			
48*E*	0.375	4.08	2.25	110.0	2.39	112.0
89*E*	0.415	3.16	3.00	100.0	2.28	90.03
			Sn			
89*E*	0.41	3.82	2.42	100.0	2.36	104.0
			Metallic-covalent bonding			
			Al			
25*SP*	0.48	3.56	2.60	77.8	2.40	109.0
50*SP*	0.56	4.56	2.78	88.0	2.47	103.0
			Ge			
71*SP*	0.41	4.56	2.73	93.0	2.53	103.0
			Sn			
25*SP*	0.46	4.18	2.80	73.0	2.60	106.0
			Metallic bonding			
			Al			
28*E*	0.39	3.78	2.38	90.2	3.72	74.8
			Germanium			
			Covalent bonding			
			Al			
51*SP*	0.43	1.91	2.70	101.0	1.80	105.0
			Metallic-covalent bonding			
			Al			
25*E*	0.24	3.30	3.34	85.0	2.09	101.0
49*SP*	0.40	3.72	3.7	77.0	2.8	91
			Sn			
25*SP*	0.48	3.58	3.16	78.7	2.70	97.0
50*SP*	0.28	3.40	3.06	87.0	2.70	95.1
			Metallic bonding			
			Al			
63*E*	0.41	3.46	2.97	97.1	2.37	80.5

nearly always from *S* to *M*. This effect, though enhanced with respect to dimers, does not show a clear dependence on the cluster size. On the contrary, the charges are only 2–3 times larger than in the dimer configuration. This figure is in reasonable agreement with the average value of the coordination and leads to an approximation for the electronic charge of the form $Q_{\rm el}=\text{coor}\times Q_{\rm dim}$, where $Q_{\rm dim}$ is the dimer charge reported in Table I(b).

B. The geometry of heteronuclear clusters: The spectra of the electronic energies and the normal modes

Our previous analysis[2] of Si and Ge clusters with Pb impurities showed that the distinction between spherical and elongated clusters survives also in heteronuclear structures. Furthermore three types of bonding were identified, i.e., covalent, metallic, and an intermediate form where one part of the cluster atoms has a metallic bond and the other part the covalent one. The grounds for such distinction was entirely geometrical as it was based on the average bond angle and bond distance having the values typical of semiconductors or of the metallic fcc structures. The results on Si and Ge clusters containing Al, Ge, and Sn as heteroatoms (Table IV) are in agreement the previous ones. As in Ref. 2, the ''metallic'' and the ''covalent'' behavior can be taken up by Si and Ge or by Al, Ge, and Sn.

The spectra of the electronic energies and the normal modes of heteroclusters are presented in Figs. 6 and 7. The comparison with the analogous quantities reported in Figs. 2 and 3 emphasizes the extreme complexity of the bond distribution within heteronuclear clusters. It is, however, observed that, if the heteroatom is of the heavier type, the maximum of

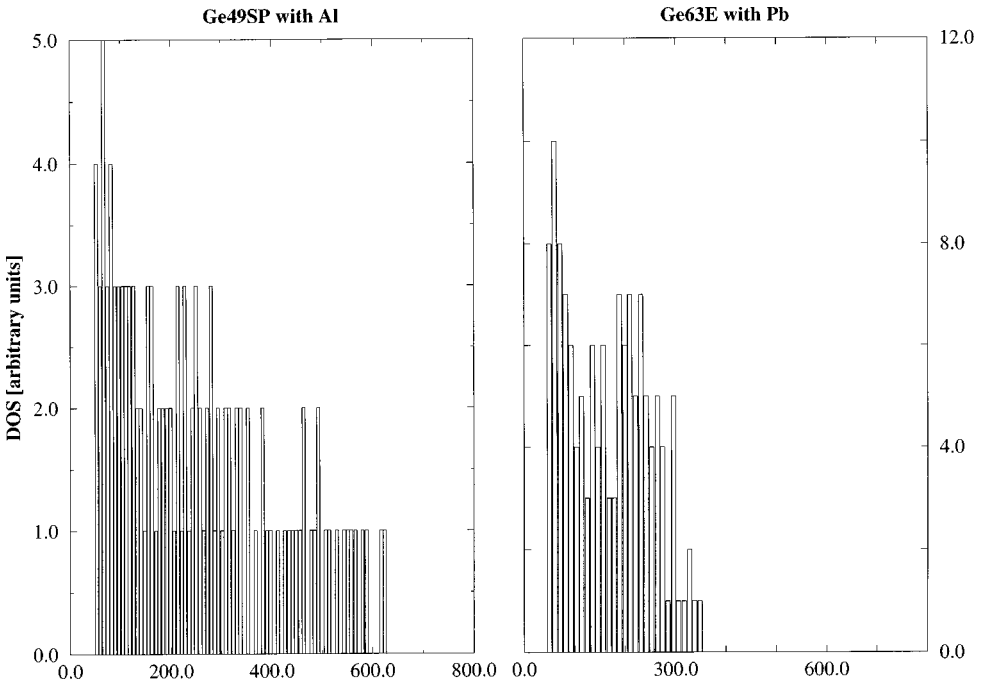

FIG. 7. The vibrational spectrum of heteroclusters. The figure shows the distribution of eigenmodes for Ge49*E* with 20 Al atoms and Ge63*E* with 14 Pb atoms.

the eigenenergies increases and that of the frequency spectrum decreases and the reverse holds for a lighter heteroatom. This behavior indicates that, in spite of the great complexity of the bond distributions, the features of a classic harmonic oscillator survive also in heteroclusters.

In agreement with these data, the temperature dependence of the entropy showed the Einstein-Debye behavior reported above in Fig. 4. However, an increase of the high-temperature limit above the homonuclear value was observed. This increase showed a critical dependence on the cluster structure and on the content of heteroatoms. As representative figures we report that the increase of entropy for clusters of size $N\sim 90$ and ~ 50, with a fraction 0.3 and 0.4 of M heteroatoms, is 2 and 1.5, respectively. A detailed analysis of these effects is left to future works.

VI. CONCLUSIONS

The conclusions of this study are at several levels. From the point of view of the calculations many properties of homonuclear and heteronuclear clusters can be satisfactorily evaluated by the LCAO methods and these properties cover a larger range than in the usual characterization of clusters.

The structure of homonuclear and heteronuclear clusters of elements of the group IV is irregular. However, a systematization is possible in terms of an aggregate of dimers. The bond length, the bandwidth of the vibrational spectrum, and the maximum values of the spectrum of the electronic energies suggest this similarity. These effects stretch further than the atoms of group IV as they apply also to Al and it can be speculated that the validity of this systematization applies to all clusters with an ''amorphous'' structure.

The inclusion of the M element in a fraction as low as 20% leads to significant changes of the geometry and of the charge distribution of homonuclear clusters. Generally, the stability of the clusters appears to increase. However, owing to the possibility of the M atom to segregate at the surface, the heteroclusters may contain more capping terminations than the homonuclear ones and this should make them highly reactive and detectable in an experiment with chemical reactants.

Owing to the nonzero entropy at room temperature the clusters appear in all cases as nonrigid. Significant effects on the melting behavior are expected to be induced by the cluster composition.

[1] N. E. Christensen and M. Methfessel, Phys. Rev. B **48**, 5797 (1993).
[2] A. M. Mazzone, Phys. Rev. B **54**, 5870 (1996).
[3] C. C. J. Roothaan, Rev. Mod. Phys. **23**, 69 (1951).
[4] M. Dupuis and H. F. King, Int. J. Quantum Chem. **XI**, 613 (1977).
[5] M. Dupuis, A. Marquez, and E. R. Davidson, HONDO 95.3, IBM Corporation, 12401.
[6] J. P. Stewart, J. Comput. Chem. **10**, 209 (1989).
[7] QCPE Catalog Number 455 and references therein.
[8] M. H. Whangbo, R. Hoffman, and R. B. Woodward, Proc. R. Soc. London, Ser. A **366**, 23 (1979).
[9] QCPE Catalog Number 571 and references therein.
[10] R. Tubino, L. Piseri, and G. Zerbi, Phys. Rev. B **56**, 1022 (1972).
[11] J. Fortner, R. Q. Yu, and J. S. Lannin, J. Vac. Sci. Technol. A **8**, 3493 (1990).

[12] M. D. Segall, R. Shah, C. J. Pickard, and M. C. Payne, Phys. Rev. B **54**, 16 317 (1996).
[13] D. Nehete, V. Shah, and D. G. Kanhere, Phys. Rev. B **53**, 2126 (1996).
[14] W. M. C. Foulkes, Phys. Rev. B **48**, 14 216 (1993).
[15] S. N. Khanna and P. Jena, Phys. Rev. Lett. **69**, 1664 (1992).
[16] T. L. Beck, D. M. Leitner, and R. S. Berry, J. Chem. Phys. **89**, 1681 (1988).
[17] I. L. Garzon and A. Posada-Amarillas, Phys. Rev. B **54**, 11 796 (1996).
[18] J. Song, S. E. Ulloa, and D. A. Drabold, Phys. Rev. B **53**, 8042 (1996).
[19] C. Rey, J. Garcia-Rodeja, and L. J. Gallego, Phys. Rev. B **54**, 2942 (1996).
[20] Y. Jinlong, W. Kelin, L. F. Dona' delle Rose, and F. Toigo, Phys. Rev. B **44**, 4275 (1991).
[21] H. Basch, M. D. Newton, and J. W. Moskowitz, Phys. Rev. B **73**, 4492 (1980).
[22] M. R. Hoare and P. Pal, J. Cryst. Growth **17**, 77 (1972).
[23] M. R. Pedersen, K. Jackson, D. V. Porezag, Z. Hajnal, and Th. Fraunheim, Phys. Rev. B **54**, 2863 (1996).
[24] M. Tegze and J. Hafner, Phys. Rev. B **39**, 8263 (1989).
[25] L. C. Balbas and J. L. Martins, Phys. Rev. B **54**, 2937 (1996).
[26] A. N. Patil, N. Otsuka, and R. P. Andres, in *Determining Nanoscale Physical Properties of Materials by Microscopy and Spectroscopy*, edited by M. Sarikaya *et al.*, MRS Symposia Proceedings No. 332 (Materials Research Society, Pittsburgh, 1994), p. 195.